Overcoming volume selectivity of dipolar recoupling in biological solid-state NMR

Zdeněk Tošner[1,4], Riddhiman Sarkar[1,3], Johanna Becker-Baldus[5], Clemens Glaubitz[5], Sebastian Wegner[6], Frank Engelke[6], Steffen J. Glaser[2], Bernd Reif[1,3]

[1] Munich Center for Integrated Protein Science (CIPS-M) at [2]Department Chemie, Technische Universität München (TUM), Lichtenbergstr. 4, 85747 Garching, Germany

[3] Helmholtz-Zentrum München (HMGU), Deutsches Forschungszentrum für Gesundheit und Umwelt, Ingolstädter Landstr. 1, 85764 Neuherberg, Germany

[4] Dept. of Chemistry, Faculty of Science, Charles University, Hlavova 8, CZ-12842 Prague 2, Czech Republic

[5] Institute for Biophysical Chemistry & Center for Biomolecular Magnetic Resonance, Goethe-University Frankfurt, Frankfurt 60438, Germany

[6] Bruker Biospin, Silberstreifen 4, D-76278 Rheinstetten, Germany

Corresponding authors:

Zdeněk Tošner tosner@natur.cuni.cz

Bernd Reif reif@tum.de

Keywords:

solid state NMR, dipolar recoupling, radiofrequency field inhomogeneity, volume selectivity, optimal control, temporal rf field modulations

Abstract

Dipolar recoupling in solid state NMR is an essential method for establishing correlations between nuclei that are close in space. In applications on protein samples, the traditional experiments like ramped and adiabatic DCP suffer from the fact that dipolar recoupling occurs only within a limited volume of the sample. This selection is dictated by the radiofrequency (rf) field inhomogeneity profile of the excitation solenoidal coil. We employ optimal control strategies to design dipolar recoupling sequences with substantially larger responsive volume and increased sensitivity. We show that it is essential to compensate for additional temporal modulations induced by sample rotation in a spatially inhomogeneous rf field. Such modulations interfere with the pulse sequence and decrease its performance. Using large scale optimizations we developed pulse schemes for magnetization transfer from amide nitrogen to carbonyl (NCO) as well as aliphatic carbons (NCA). Our experiments yield a signal intensity increased by a factor of 1.5 and 2.0 for NCA and NCO transfers, respectively, compared to conventional ramped DCP sequences. Consistent results were obtained using several biological samples and NMR instruments.

Main text

Experimental sensitivity is the major obstacle in applications of solid state nuclear magnetic resonance (NMR) in structural biology[1]. In studies of protein samples, correlations of chemical shifts between amide nitrogen and carbon atoms of the protein backbone are essential for resonance assignments[2]. For this purpose, dipolar recoupling methods are employed. In the basic variant of the double cross polarization (DCP) experiment[3], a resonant radiofrequency (rf) field is applied to both the ^{15}N and ^{13}C nuclei which interferes with the spatial rotation of the sample (magic angle spinning, MAS) and re-introduces the direct dipole-dipole interaction. For an efficient magnetization transfer, the rf amplitudes have to satisfy the Hartman-Hahn (HH) condition[4] ($\omega_N \pm \omega_C = n\omega_R$, where $\omega_R/2\pi$ is the sample spinning frequency, ω_N and ω_C are the rf amplitudes on the ^{15}N and ^{13}C channels respectively, expressed in rad/s, and $n = \pm 1, \pm 2$). However, due to rf field inhomogeneities imposed by the NMR coil the HH condition cannot be fulfilled for the whole volume of the sample and it leads to a loss of sensitivity. The most widely used experiments today are the ramped and adiabatic DCP[5] in which the rf amplitude on one of the rf channels is modulated and swept through the HH condition. Experimentally, the efficiency of the DCP experiment is evaluated as the ratio of the signal intensities of the ^{13}C CP-MAS spectrum and the DCP spectrum. The current standard efficiency of the ramped/adiabatic DCP experiment is 30-40% when a rotor is completely filled with sample, and about 65% when the sample is restricted to the central slice of the rotor where the rf field is expected to be homogeneous[6]. It is obvious that the experiment does not work equally well for the whole sample volume and it is estimated that 30-50% of the sample remains NMR silent[7]. This fact is documented in Figure 1 where one-dimensional images of the sample acquired in the presence of static field gradient are compared. When a ^{13}C hard pulse is used for excitation, the width of the image is much larger compared to the DCP experiment. Recoupling is only effective within the central region of the sample where rf fields are relatively homogeneous, while the other parts of the sample yield no signal. Recently, an improved robustness towards rf inhomogeneity and rf amplitude mismatch was achieved using the RESPIRATION-CP method[6]. The recoupling element consists of a phase-alternating constant amplitude rf field which is applied to only one channel while it is simultaneously interleaved with strong pulses on both channels. This experiment provided an 80% increase of signal compared to adiabatic DCP at a spinning frequency of 30 kHz and using a 3 ms contact time. Using numerical simulations, the problem associated with volume selection is delineated further in supplementary Figure S-1. The performance of ramped, adiabatic, RESPIRATION as well as optimal control DCP sequences is evaluated as a function of the position of the sample along the 3.2mm rotor axis. These images provide strong motivation for development of improved pulse sequences.

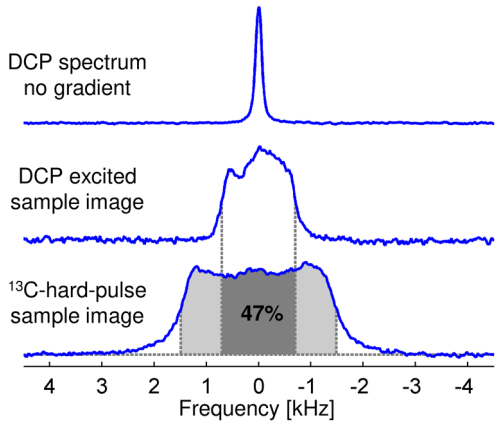

Figure 1. Volume selectivity of the DCP experiment. Experimental ^{13}C NMR spectrum of $^{13}C_2$,^{15}N-glycine obtained using ramped DCP excitation (top), the same experiment performed in the presence of a static magnetic field gradient along the sample axis, which produces a one-dimensional image of the sample (middle), and ^{13}C sample image acquired under the same gradient but using a hard pulse for excitation (bottom). It is evident that dipolar recoupling during DCP was efficient only within the central part of the sample, yielding only 47% excitation of the available sample volume. All spectra were acquired at a MAS frequency of 30 kHz using a 1.9 mm MAS probe with the gradient coil. See also supplementary Figure S-1 presenting selectivity for other pulse sequences based on numerical simulations.

In this work, we focus on application of optimal control (OC) tools[8] for the design of new pulse sequences with improved robustness towards rf inhomogeneity. The optimal control problem is defined as a state-to-state transfer of magnetization from ^{15}N to ^{13}C for a prototypical spin system that reflects the relevant experimental conditions. A numerical optimization protocol is set up to find amplitudes and phases of element pulses that constitute the total pulse sequence and provide the maximal transfer efficiency. Optimal control theory provides easy access to the first derivative of the objective function and allows to optimize tens of thousands of variables at once. Since the first application of OC to the DCP experiment[9], two other studies have been published by Kehlet *et al*.[10] and Loening *et al*.[11] When performance of these sequences was tested experimentally, only minor improvements compared to adiabatic DCP were observed. Clearly, there is a discrepancy between the experimental implementation and the theoretical model that predicted about 2-fold increase of sensitivity.

In both studies, a rather limited range of rf fields was used during optimization. The relative rf amplitudes were assumed to vary by about $\pm$10% around the nominal value. This range was sufficient to simplify the experimental setup but it is not large enough to cover all situations inside a typical solenoidal coil which is used in MAS probes. Along the coil axis, the rf amplitude is reduced to 50% at the ends of a coil compared to the center (supplementary Figure S-1). Recently, it was suggested to fit the rf field profile using an empirical power-law formula and to determine its parameters experimentally by evaluation of a nutation experiment[12]. However, such a model is still too simplistic. It turns out that the rf field distribution in all three spatial dimensions and for the whole sample volume needs to be considered. Sample rotation introduces periodical modulations of the rf amplitude and phase. Under MAS, a given spin packet in a certain volume element travels along a circle and

experiences variable rf fields. The variations depend on the position along the coil axis as well as on the radial distance from the coil axis[7]. The modulations become particularly important for regions at the surface of the MAS rotor and near the end of the coil, where the relative rf amplitude fluctuates up to ±25% and the rf phase changes by up to ±30°. It is important to realize that most of the sample material is located at the walls of the rotor and not in the center. The effect of radial rf inhomogeneities on solid-state NMR spectra has been realized already many years ago[13]. However, so far it was not possible to compensate for these periodic rf field modulations that interfere with the pulse sequence.

For the purpose of demonstration, the sample volume of a thin-walled 3.2 mm MAS rotor is divided into 3 coaxial layers of equal thickness but of different volumes (Figure 2A). The position of a given volume element is described using cylindrical coordinates (z, r, ϑ) where z describes the position along the rotor axis (and which is assumed to be identical to the coil axis), r is the radial distance and ϑ refers to the azimuthal angle. The spins in the volume elements which are located at different azimuthal angles ϑ experience rf field modulations with a different initial phase. The total Hamiltonian that governs the spin dynamics (that is the dipole-dipole interactions and the rf irradiation) is homogeneous in the sense of Maricq and Waugh[14], i.e. it does not commute with itself at different times. Therefore the spins with different angle ϑ undergo different dynamics, the effect of rf inhomogeneity is different. If the calculation assumes an OC pulse sequence which compensates only for rf field inhomogeneity along the coil axis, we find that the transfer efficiency is small in a large fraction of the sample (Figure 2B).

To generate pulse sequences whose performance is not influenced by rotational modulations of the rf field, a complex optimal control protocol was devised. In the following, we refer to the method as tm-SPICE, standing for temporally modulated SPatial rf field Inhomogeneity CompEnsation. The sample volume was divided into elements for which the rf field was calculated assuming a solenoidal coil as described in our previous work[7]. The actual values are provided in the Supporting material (Tables S-1, S-2). The rotational rf field modulations were ignored for the inner layer while for the other volume elements the pulse sequence amplitudes and phases were adjusted to reflect the local rf fields as they change with time. The modified rf Hamiltonian and the corresponding gradient of the propagator operator that are necessary for the OC optimization are presented in the Supporting material (section 4). The total duration of the sequence was set to 3.5 ms and was digitized using 2 μs time steps, resulting in 7000 free variables (amplitudes and phases on two rf channels). The MAS frequency was set to 20 kHz. Parameters for powder averaging, dispersion of ^{13}C and ^{15}N chemical shifts, and spatial rf field inhomogeneity resulted in 54 600 different conditions that the OC sequence has to fulfill simultaneously. The computation demands are magnified by the need of performing 4-spins simulations to secure robustness towards different spin systems (vide infra). The calculations were implemented in the SIMPSON software[15] and typically required about 4 days per optimization when using 200 Intel Xeon computer cores. More details about the calculation are provided in the Supporting material. The optimization was repeated 5 times for each NCA and NCO magnetization transfers in order to test for possible local minima traps. The typical performance of the resulting tm-SPICE CP pulse sequence in the whole sample volume is documented in Figure 2C showing that the effect of rotational modulations of the rf field is compensated.

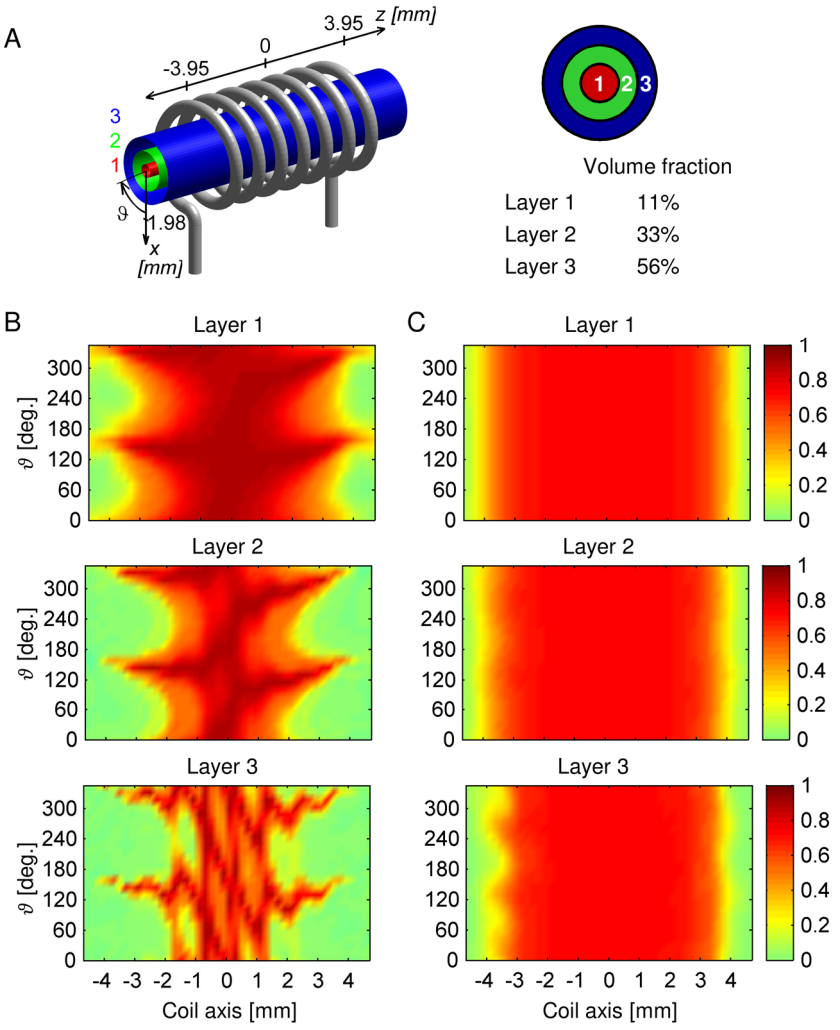

Figure 2. Performance of OC CP sequences calculated on the basis of individual volume elements for a NCA transfer. (A) The sample volume is divided into layers 1, 2 and 3 of equal thickness but different fractions of the total volume. (B) Performance of the OC CP sequence optimized assuming a rf field distribution only along the coil axis. The transfer efficiency differs significantly for individual volume elements in the different layers. While the performance is good along the rotor axis (layer 1), it is very low due to rf modulations imposed by sample rotation in layer 3. (C) Performance of the final tm-SPICE CP sequence optimized taking into account a full 3D rf field distribution including temporal modulations of rf field amplitudes and phases. A high transfer efficiency is obtained in all 3 layers.

Loening et al.[11] discuss the deficiency of the OC sequences that are optimized using a two-spin model. In their case the efficiency of the NCA transfer drops down to about a half when it is applied to a 5-spin system including the nearby carbon atoms and assuming a fully labeled protein. We find that this problem can be removed when the optimizations assume a four-spins system consisting of N, Cα, C', Cβ and Cα, C', N, Cα for NCA and NCO transfers, respectively. Our tm-SPICE CP yields almost equal performance when applied to different spin systems comprising 2-5 nuclei (supplementary Figure S-2).

Another objection against OC pulse sequences relates to pulse transients[16]. Rapid switching of amplitudes and phases cannot be followed exactly by the NMR hardware due to the finite bandwidth of its rf circuits. As a consequence, the actual shape of a pulse is distorted. We used a Bruker $^{1}H,^{13}C,^{15}N,^{2}H$ 4-channel MAS probe with the ^{2}H channel realized using a secondary rf coil. This coil was used as a pick-up system for direct observation of rf irradiation and to visualize the exact shapes of the OC pulse sequences. The experimental details are summarized in the Supporting material (section 3). In addition to the transients that occur at a switch of amplitude or phase, we observe small variations of the absolute value of amplitudes and phases when a pulse is applied repeatedly during a sequence. This additional effect is presumably due to amplifier instabilities during the pulse sequence. Nevertheless, in our measurements we found that the amplitudes did not differ more than 2% and the phase was reproduced with 5° accuracy. The distorted pulses were used in numerical simulation of the transfer efficiency and compared to the original sequence with perfectly rectangular pulses. It was found that transients and amplifier effects decreased the performance of the OC sequences by less than 10%. Optimal control pulse sequences are not periodic and do not seem to be largely influenced by pulse transients. This is in contrast to symmetry-based recoupling sequences for which the pulse imperfections lead to an additional effective field that alters the recoupling condition[17]. While it is possible to include transients in optimal control protocol [16c], no effort was made to compensate for them in our calculations.

The resulting tm-SPICE CP pulse sequences were tested experimentally using several microcrystalline samples including a MLF tripeptide, the α-spectrin SH3 domain, aβ-amyloid fibrils and a proteoliposoms sample of the membrane protein Diacylglycerol kinase (DGK). Several NMR instruments were used, with proton Larmor frequencies of 400, 500, 750 and 900 MHz. More details are given in the Supporting material (section 6). To date, ramp and adiabatic DCP[5] are widely used for ^{15}N to ^{13}C transfers in biological samples. To obtain good transfer efficiencies, both versions of the experiment have to be carefully optimized with respect to the shape, rf amplitudes and offsets. Using a contact time of 3.5 ms and a MAS frequency of 20 kHz, we obtained a similar performance for both of the two optimized experiments. We therefore decided to use the widely employed ramp 90-100% for all reference experiments. The variation by changing the DCP sequence is much smaller than the observed improvement using tm-SPICE CP. We consistently observe more than a 2-fold increase of the signal amplitude for the NCO transfer and about a 1.5-fold increase for the NCA transfer when compared to the ramp DCP experiment. The spectra of the DGK membrane protein are compared in Figure 3 while the other experimental results are included in supplementary Figure S-8. In the case of the NCO experiment our results agree very well with numerical predictions. The transfer efficiency of ramp DCP and tm-SPICE CP was calculated using the 3D maps of the rf field distribution as it is described in Supplementary material (section 7). The predicted signal improvement factor of 2.22 agrees perfectly with our experimental observations. The efficiency of the NCA transfer is compromised presumably by strong dipolar couplings to the surrounding protons. To evaluate the influence of remote protons, the signal intensity of the tm-SPICE CP experiment was measured as a function of the proton decoupling strength using the MLF sample (supplementary Figure S-9A). We observe that the signal increases till the hardware limit for ^{1}H decoupling power is reached (about 110 kHz). We performed numerical simulations assuming a 7-spins system consisting of the nuclei N, Cα, Cβ together with the 4 closest protons (HN, Hα, Hβ1, Hβ2), accounting for rf field inhomogeneities on all 3 rf channels along the coil axis. The results suggest that the performance of the sequence is reduced to

67% in comparison to the theoretical maximum, in case only 100 kHz proton decoupling is employed (supplementary Figure S-9B). Taking into account the reduced performance due to insufficient proton decoupling we arrive at a theoretical signal enhancement factor of about 1.57 which again agrees perfectly with the experiment.

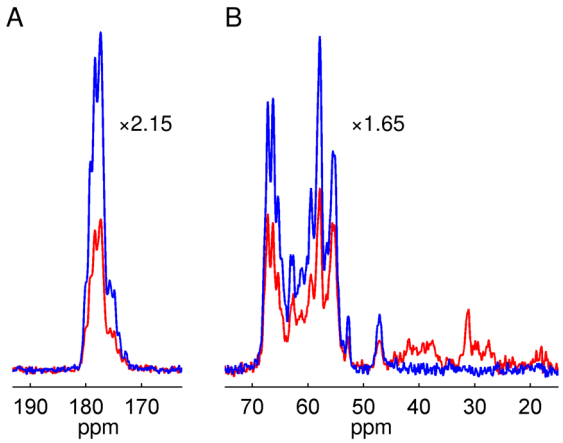

Figure 3. Experimental tm-SPICE CP spectra (blue) compared to standard ramped DCP spectra (red) measured for the membrane protein diacylglycerol kinase DGK. (A) The NCO experiment yields two times more signal. (B) In addition to the gain of 1.6 in sensitivity, the NCA experiment provides better selectivity as no Cβ signals are observed. In the experiment, a 3.5 ms contact time and a MAS frequency of 20 kHz has been employed. The measurement was carried out at a magnetic field strength of 21.1 T.

It is interesting to closely inspect the tm-SPICE CP pulse sequence. In Figure 4 the rf fields are represented separately for their ω_x and ω_y components. To a large extent, the rf field of the shapes is synchronously modulated with sample rotation. Effectively, one pulse is applied every rotor period (50 μs). Other representations of the pulse sequences as well as their electronic form are provided in the Supporting material (section 5). While we still lack a detailed understanding on the level of effective Hamiltonian, we can identify some of the concepts used in analytically derived pulse sequences. For example, the phase of pulses on the ^{13}C channel at the end of the NCO tm-SPICE CP sequence (Figure 4D, time 2.6 – 3.5 ms) is changed from –x to +x in the XiX fashion. The fragment of the NCA sequence between times 1.0 and 1.3 ms (Figure 4A,B) strongly resembles the RESPIRATION-CP pulse sequence with fast XiX pulses on the ^{15}N channel synchronized with strong y-phase pulses on the ^{13}C channel. It is interesting to see that this motif is present for the next 0.3 ms, with only the role of the ^{15}N and the ^{13}C channel being swapped. Like in the case of RESPIRATION-CP[6], the outcome of the numerical optimizations might serve in the future as an inspiration for the analytical development of pulse sequences. Generally, we observe more synchronization and a clearer structure in the optimal control pulse sequences when the optimization is performed only for a single set of conditions. The more conditions that have to be fulfilled simultaneously, the more complex the optimized shape will be.

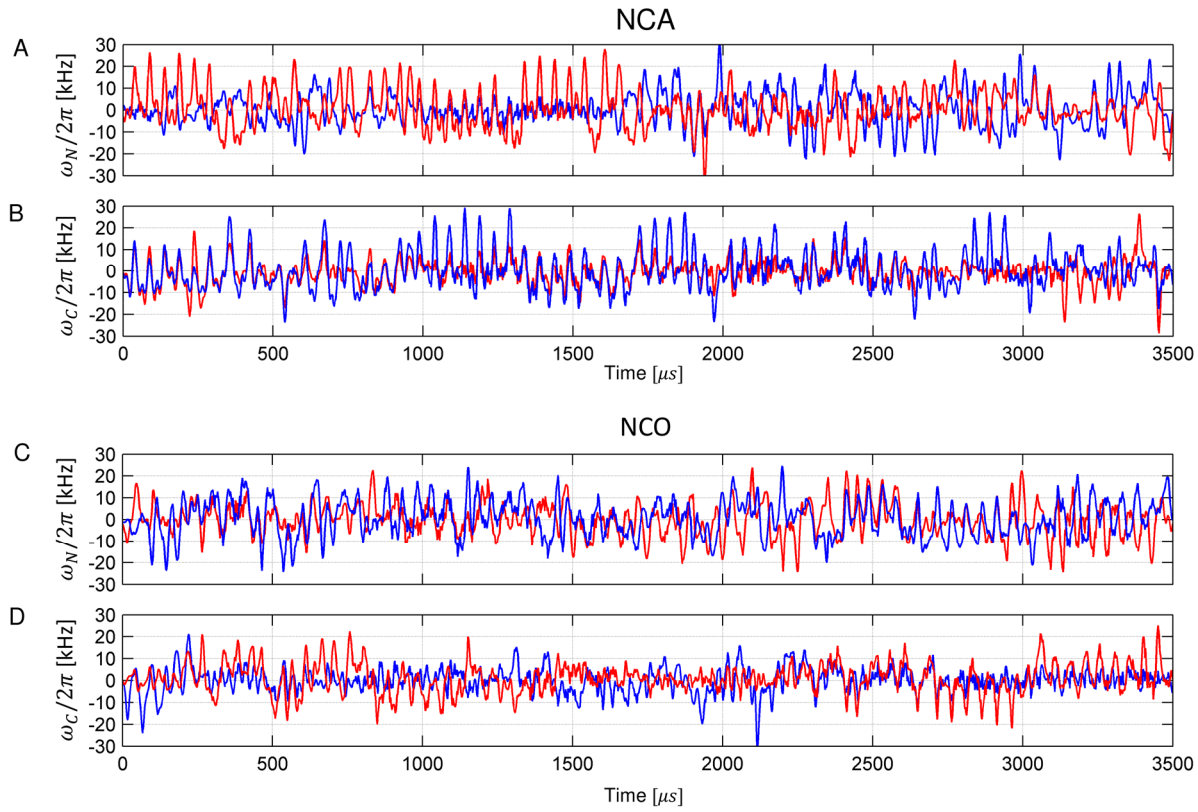

Figure 4. tm-SPICE CP pulse sequences for NCA (panels A, B) and NCO (panels C, D) transfers. The rf pulses are presented using their ω_x (red) and ω_y (blue) components for the ^{15}N channel (panels A, C) and the ^{13}C channel (panels B, D), respectively. The maximal rf amplitude is below 35 kHz and the average is below 10 kHz for all shapes. The duration of all pulses was fixed to 2 μs.

In conclusion, we have shown that optimal control can provide pulse sequences that greatly increase the NMR responsive sample volume. It is crucial to take into account the 3D distribution of the rf field inside the NMR coil. Due to sample rotation, the rf fields for a given sample volume fluctuate significantly both in their rf amplitudes and phases which can strongly influence the performance of the pulse sequence. We have shown that OC pulse sequences can be designed for prototypical spin systems that are encountered in biological solids such as uniformly labeled proteins. We find that their performance is not altered significantly when the spin labeling scheme is changed. Similarly, the performance does not depend on the size of static magnetic field or construction details of the NMR probe. Our data clearly demonstrates the transferability of the sequences among spectrometers. Re-optimization for different magnetic fields is not necessary as long as a MAS frequency of 20 kHz and a contact time of 3.5 ms are used. Although the OC sequences may involve elements with rapid amplitude and phase changes, pulse transients and small amplifier instabilities do not seem to affect the performance of the heteronuclear dipolar recoupling in these experiments. We find that the observed 1.5-fold to 2.0-fold increase in signal intensity of the tm-SPICE CP experiment is a consequence of the exploitation of a larger fraction of the sample volume. When volume restricted samples are used (i.e. center packed samples) the tm-SPICE CP experiment performs equally in comparison with the ramped DCP. We anticipate that experimental techniques that make use of the

full volume of the available sample are crucial for the future of solid state NMR where the sensitivity of the experiment is limiting.

Acknowledgement

This project received funding from the European Union's Horizon 2020 research and innovation program under the Marie Sklodowska-Curie grant agreement No 657682. In addition, we are grateful to the Helmholtz-Gemeinschaft, the Deutsche Forschungsgemeinschaft (Grants Re1435, Gl 203/7-2 and SFB-1035, project B07), and to the Center for Integrated Protein Science Munich (CIPS-M) for financial support. Access to computing facilities of the Czech National Grid Infrastructure MetaCentrum provided under the program "Projects of Large Research, Development, and Innovations Infrastructures" (CESNET LM2015042), and access to the computational resources of Leibnitz Supercomputing Center is greatly appreciated. We thank Julian de Mos and Christian Bonifer for kindly providing the sample of DGK.

Supporting material

Extensive supporting material is provided that includes all experimental details regarding transient effect measurements, tm-SPICE CP measurements, as well as all SIMPSON simulations and optimizations. The pulse shapes are provided in electronic form (Bruker shape format).

References

[1] J. H. Ardenkjaer-Larsen, G. S. Boebinger, A. Comment, S. Duckett, A. S. Edison, F. Engelke, C. Griesinger, R. G. Griffin, C. Hilty, H. Maeda, G. Parigi, T. Prisner, E. Ravera, J. van Bentum, S. Vega, A. Webb, C. Luchinat, H. Schwalbe, L. Frydman, *Angewandte Chemie-International Edition* **2015**, *54*, 9162-9185.

[2] A. E. McDermott, *Current Opinion in Structural Biology* **2004**, *14*, 554-561.

[3] J. Schaefer, R. A. McKay, E. O. Stejskal, *Journal of Magnetic Resonance (1969)* **1979**, *34*, 443-447.

[4] S. R. Hartmann, E. L. Hahn, *Physical Review* **1962**, *128*, 2042-2053.

[5] M. Baldus, D. G. Geurts, S. Hediger, B. H. Meier, *Journal of Magnetic Resonance Series A* **1996**, *118*, 140-144.

[6] S. Jain, M. Bjerring, N. C. Nielsen, *J. Phys. Chem. Lett.* **2012**, *3*, 2020-2020.

[7] Z. Tošner, A. Purea, J. O. Struppe, S. Wegner, F. Engelke, S. J. Glaser, B. Reif, *Journal of Magnetic Resonance* **2017**, *284*, 20-32.

[8] N. Khaneja, T. Reiss, C. Kehlet, T. Schulte-Herbruggen, S. J. Glaser, *Journal of Magnetic Resonance* **2005**, *172*, 296-305.

[9] C. T. Kehlet, A. C. Sivertsen, M. Bjerring, T. O. Reiss, N. Khaneja, S. J. Glaser, N. C. Nielsen, *Journal of the American Chemical Society* **2004**, *126*, 10202-10203.

[10] C. Kehlet, M. Bjerring, A. C. Sivertsen, T. Kristensen, J. J. Enghild, S. J. Glaser, N. Khaneja, N. C. Nielsen, *Journal of Magnetic Resonance* **2007**, *188*, 216-230.

[11] N. M. Loening, M. Bjerring, N. C. Nielsen, H. Oschkinat, *Journal of Magnetic Resonance* **2012**, *214*, 81-90.

[12] R. Gupta, G. Hou, T. Polenova, A. J. Vega, *Solid State Nucl Magn Reson* **2015**, *72*, 17-26.

[13] a) T. G. Oas, R. G. Griffin, M. H. Levitt, *The Journal of Chemical Physics* **1988**, *89*, 692-695; b) P. Tekely, M. Goldman, *Journal of Magnetic Resonance* **2001**, *148*, 135-141.
[14] M. M. Maricq, J. S. Waugh, *The Journal of Chemical Physics* **1979**, *70*, 3300-3316.
[15] a) M. Bak, J. T. Rasmussen, N. C. Nielsen, *Journal of Magnetic Resonance* **2000**, *147*, 296-330; b) Z. Tošner, T. Vosegaard, C. Kehlet, N. Khaneja, S. J. Glaser, N. C. Nielsen, *Journal of Magnetic Resonance* **2009**, *197*, 120-134; c) Z. Tošner, R. Andersen, B. Stevenss, M. Eden, N. C. Nielsen, T. Vosegaard, *Journal of Magnetic Resonance* **2014**, *246*, 79-93.
[16] a) M. Mehring, J. S. Waugh, *Review of Scientific Instruments* **1972**, *43*, 649-653; b) T. M. Barbara, J. F. Martin, J. G. Wurl, *Journal of Magnetic Resonance (1969)* **1991**, *93*, 497-508; c) P. E. Spindler, Y. Zhang, B. Endeward, N. Gershernzon, T. E. Skinner, S. J. Glaser, T. F. Prisner, *Journal of Magnetic Resonance* **2012**, *218*, 49-58.
[17] a) J. J. Wittmann, K. Takeda, B. H. Meier, M. Ernst, *Angewandte Chemie* **2015**, *54*, 12592-12596; b) J. J. Wittmann, V. Mertens, K. Takeda, B. H. Meier, M. Ernst, *Journal of Magnetic Resonance* **2016**, *263*, 7-18.